

Tomographic identification of gas bubbles in two-phase flows with the combined use of the algebraic reconstruction technique and the genetic algorithm

Ken D. Kihm, H. S. Ko, and Donald P. Lyons

Department of Mechanical Engineering, Texas A&M University, College Station, Texas 77843-312

Received January 20, 1998

Combined use of the algebraic reconstruction technique (ART) and the genetic algorithm (GA) shows highly accurate and efficient tomographic reconstruction of line-of-sight projection images of two-phase flows compared with reconstructions obtained by separate use of these methods. A modified GA-based tomography uses the ART reconstruction result as preliminary information on the number, shapes, and sizes of bubbles to be reconstructed. This combined use of the two methods exploits faster convergence of the ART to the approximate solution space and more robust and accurate optimization of the GA to the ultimate solution space. In the investigation a computer-synthesized phantom field that consisted of five elliptical gas bubbles in liquid or solid surroundings was used. © 1998 Optical Society of America

OCIS codes: 110.6960, 200.1130, 280.2490, 100.0100.

Two-phase flows, such as bubbly liquid flows or solidladen liquid flows, are popular in many industrial processes, and the nonintrusive determination of the number, locations, and sizes of the bubbles (or solid particles) is increasingly in demand to monitor the component fractions and their distributions. The line-of-sight optical projection of two-phase flows is expressed as a line integral of the wave impedance $I(x, y)$ along the ray occupied by the test field (Fig. 1), i.e.,

$$\psi(r, \phi) = \iint I(x, y) \delta(r - x \cos \phi - y \sin \phi) dx dy \quad (1)$$

where $\delta(\dots)$ denotes the Dirac delta function. The projection Ψ and the impedance I are specified for an optical technique to be considered (Table 1).

For simplicity, here the projection is an algebraic integral of the medium (gas, liquid, or solid) density along the ray, and the impedance is identical to the density field, i.e., $I(x, y) \equiv \rho(x, y)$. One must reconstruct the impedance or density field from the measured projection data Ψ by inverting the integral of Eq. (1). This numerical data processing is called tomography.

For illustrative purposes, a phantom density field is chosen as a summation of five elliptical bubbles [Fig. 2(a)]. Thus the j th bubble is described as an elliptical function g_j :

$$g_j(x, y; A_j) = \begin{cases} 1 & \left(\frac{x - x_j}{a_j} \right)^2 + \left(\frac{y - y_j}{b_j} \right)^2 \leq 1 \\ 0 & \text{otherwise} \end{cases} \quad (2)$$

where $A_j = (x_j, y_j, a_j, b_j)$, whose components correspond to the location coordinates of the center and the major and minor axes of the ellipse. Binary basis function values are given to represent a normalized field impedance (density) of 1 for the region inside the bubble and of 0 for liquid or solid outside the bubble.

The line-of-sight projection, Eq. (1), is known mathematically as the Radon transform^{1,2} of function $I(x, y)$, and the Radon transform is a function of the projection plane coordinate r and the projection angle ϕ in Fig. 2(b), as shown for the Radon transform of the phantom field [Fig. 2(a)]. An accurate mathematical inversion of Eq. (1) can be obtained only if the inverse Radon transform is known for all $\Psi(r, \phi)$ and infinitely many projections are available for infinitely many projection angles ϕ . Since the inverse Radon transformations of most asymmetric impedance functions are not available and only a finite number of projections are allowed in practice, a two-dimensional Fourier inversion, instead of the direct inversion by Radon transformation, is used to achieve an approximate inversion of Eq. (1). Nevertheless, the Fourier inversion requires a significant number of equally angled projections for acceptable accuracy and mathematical stability.

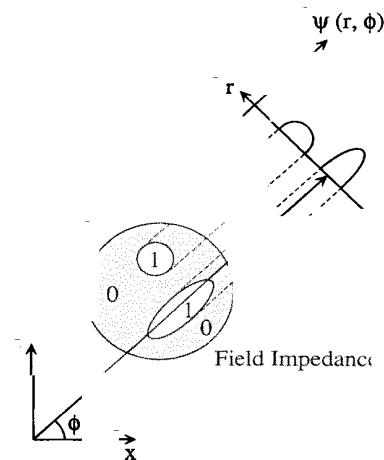


Fig. 1. Line-of-sight optical projection of two-phase impedance field.

Table 1. Examples of Line-of-Sight Projection Ψ and Impedance I for Different Optical Techniques

Technique	Ψ	I
Interferometry	Fringe pattern	Density field
Speckle photography	Beam deflection angle	Lateral gradient of density field
X-ray computerized tomography or γ -ray	Light attenuation	Density field
Ultrasonic (nonoptical)	Pressure-wave travel time	Density function (speed of sound)

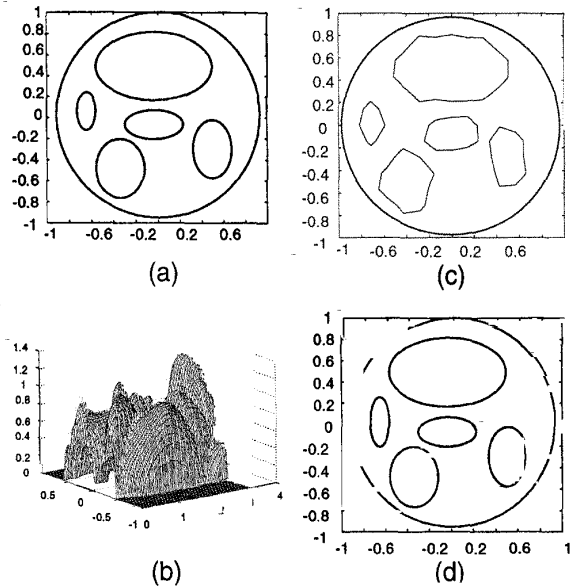


Fig. 2. (a) Computer-synthesized two-phase field, (b) its line-of-sight (Radon transform) projection, (c) image reconstructed with ART, and (d) image reconstructed by the combined use of the ART and the GA.

The alternative reconstruction algorithm to the Fourier inversion, particularly for a limited number of projections, is known as the algebraic reconstruction technique⁴ (ART). The ART constructs the field with a finite number of square pixels, and each pixel carries a randomly assigned initial pixel value A_i of either 1 (gas) or 0 (liquid or solid). The optical projection Eq. (1) of this initial estimated field generates a virtual projection ψ' . Then, by use of feedback information on the deviation of the virtual projection ψ' (from the measured projection ψ (from the true field)), iterative updating of each A_i is carried out.

Successive iterations are carried on until the feedback deviation falls within a specified convergence or meets a specified number of iterations. The algebraic update is described by

$$A_i^{q+1} = A_i^q + W_i^q \frac{\sum_p (\psi_p - \psi'_p)}{NP} \quad (3)$$

where W_i is the weighting factor, q denotes the q th iteration, P represents the number of projection angles, and N is the number of data realizations on each projection plane. Note that the ART update is possible for only a single set of unknowns (A_i) and for a linear projection that allows the algebraic updating of Eq. (3). This simplicity and linearity make the ART iteration extremely fast.

Figure 2(c) shows the field reconstructed by use of the ART, where the field is described by 15 x 15 square pixels with 225 unknown A_i ($i = 1, 2, 3 \dots 225$). In the calculation 15 equally angled projections ($P = 15$) and 15 rays ($N = 15$) per projection were used. The calculation was stopped at approximately 650 iterations, beyond which the convergence was nearly saturated. Although the calculation converges fast, the reconstruction deficiency is apparent from the use of finite square pixel representation of the field. The reconstructed bubble images roughly identify elliptical shapes. On the other hand, the ART provides the precise number of bubbles and their approximate sizes and locations. This suggests that the ART reconstruction result can be used as intelligent initial information for more sophisticated and time-consuming reconstruction algorithms, such as the genetic algorithm- (GA-) based reconstruction.⁵

The adoption of GA optimization for image reconstruction showed fairly good potential for improvement, particularly when multiple sets of unknowns had to be simultaneously optimized." One distinct advantage of GA-based reconstruction over the ART is that the former permits the use of any arbitrary type of basis function whose summation conforms to the density field to be reconstructed. In addition, the basis function can have as many parameters as necessary, since the GA-based tomography can simultaneously handle multiple sets of unknowns. The most obvious choice of the present example, reflected from the preliminary ART solution, will be five elliptical-type basis functions.

The GA-based algorithm (Fig. 3) starts with a number of solution candidates (individuals, I_i), and each individual carries four different kinds (corresponding to the x - y coordinates and the major and minor axes of the ellipse) of the total of 20 randomly assigned numbers (genes) for five bubbles. The idea of multiple solution candidates is called an implicit parallelism, and the group of individuals is called the population. The individuals and their genes evolve under the principle of guided random selection based on the survival of the fittest. The individual's fitness level enforces the survival of the fittest feature. Thus fitness (F_i) for the present example is defined as the degree of deviation of the virtual projection of an individual solution candidate and the measured projection from the true field, where the smallest fitness value is the best.

The heart of the routine is the selection of the fittest from a pool (population) of solution candidates (individuals). The selection routine picks individuals from the population, and a higher probability of selection is given to individuals with smaller fitness values. When a pair of individuals has been selected as parents 1 and 2, they are given a prespecified

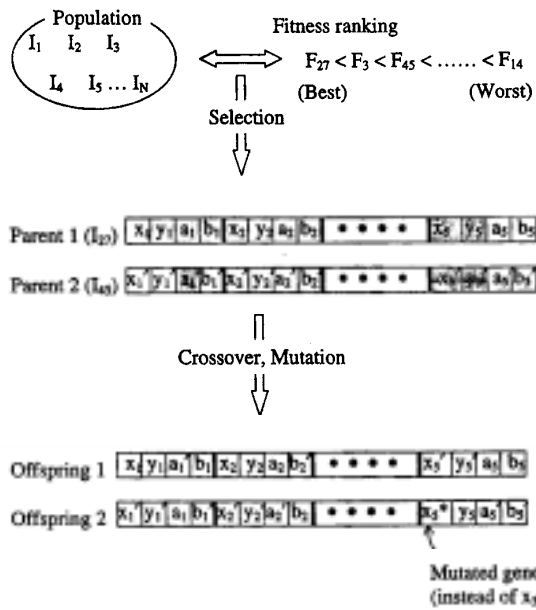


Fig. 3. Schematic illustration of the genetic operators by biased random selection, crossover, mutation, and creation of offspring.

Table 2. Comparison of Features of the ART and GA-Based Reconstruction

ART	GA-Based Tomography
Number of bubbles and approximate bubble shapes and locations are quickly available.	Accurate reconstruction of bubble shapes and sizes possible by use of an appropriate type of basis function.
Linear optimization restricted to a single set of parameters: the algorithm is simple and fast.	Nonlinear optimization allows multiple sets of parameters: the method is robust but requires lengthy computation.
Large number of total unknowns identical to the total number of pixels: $15 \times 15 = 225$.	Fewer total unknowns: $5 \text{ (bubbles)} \times 4 \text{ (} x, y \text{ locations and major/minor axes)} = 20$.

chance of creating offspring. If offspring are created, each transfer of genetic material carries a prespecified chance of a mutation of itself. It is this mutation operation that is the primary source of robustness in the algorithm. By including new genetic material in the population, the algorithm continually searches new areas of the search space for the ultimate optima in a multi-peaked problem.

One additional source of robustness is called elitism, in which any offspring and mutants do not survive unless they are better than their parents. This mechanism ensures that the best individual holds its title until a better individual evolves, so the present solution quality can be maintained for at least the next generation.

The GA-based reconstruction result of Fig. 2(d) was obtained by use of a population of 100 individuals evolving to 1000 generations with 50% crossover prob

ability and 10% mutation probability. The number of projections and the number of rays per projection as considered for the ART calculation are both 15. This GA result shows much more accuracy than the ART result.

As expected, the GA's simultaneous handling of multiple sets of parameters requires a massive amount of computation and demands 2-3 orders of magnitude more CPU time than the ART. At the cost of increased computation effort, the GA-based tomography reconstructs far more accurate shapes and locations of the bubbles. The preliminary ART calculation plays an important role in determining the number of bubbles, the rough bubble shapes, and the ballpark bubble locations in the GA. The approximate bubble shapes provide a valuable clue to the type of basis function to be selected, and at least one individual of the initial population carries genes containing the information on the ART-determined bubble locations (x, y) and sizes (a, b), so this prestigious individual can lead the evolution and significantly expedite the convergence. If the GA were used without the preliminary bubble information, its CPU time could be several times longer. The CPU time taken by the GA increases geometrically with the number of unknown parameter sets.

The ART method converges to a nearly unique solution, regardless of its initial guess as to solution field. The GA-based method, however, is a statistical method that can result in different solutions, depending on the calculation procedures. After several trials, the best solution (individual) must be selected to give the highest fitness (the lowest fitness value) or the most accurate reconstruction. The way to ensure the repeatability of the GA method is to specify a fixed random number seeder, that is, a lengthy series of random numbers, that controls each manipulation step. One must examine several different random number seeders to select the best seeder, which gives the highest reconstruction accuracy. Although this additional effort of the GA in determining the best available solution seems cumbersome and detrimental, it is commonly required in most statistical iterative methods. Table 2 summarizes a comparison of the individual ART and GA techniques, emphasizing the potential merit of their combined use.

References

1. J. Radon, *Math. Phys. Min.* 29, 262 (1917).
2. S. R. Deans, *The Radon Transform and Its Applications* (Wiley, New York, 1983).
3. A. C. Kak and M. Slaney, *Principles of Computerized Tomographic Imaging* (Institute of Electrical and Electronics Engineers, Piscataway, N.J., 1987), Chap. 3.
4. R. Gordon, *IEEE Trans. Nucl. Sci.* 21, 78 (1974).
5. D. E. Goldberg, *Genetic Algorithms in Search, Optimization, and Machine Learning* (Addison-Wesley, New York, 1989).
6. D. Tauru, K. Okamoto, H. Madarame, and M. Fumizawa, Fourth Fluid Control, Measurement and Visualization Conference, Toulouse, France, August 30-September 1.
7. K. D. Hihm and D. P. Lyons, *Opt. Lett.* 21, 1327 (1996).
8. D. P. Lyons and K. D. Hihm, *Opt. Lett.* 22, 847 (1997).